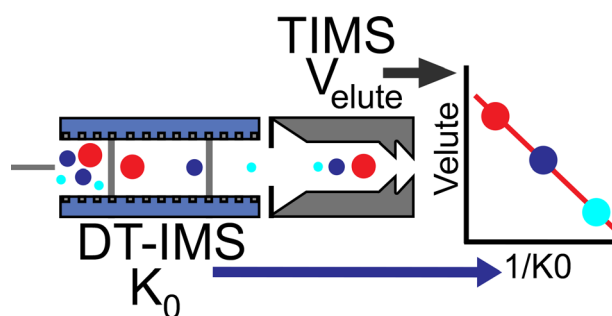Check for updates

RESEARCH ARTICLE

Validation of Calibration Parameters for Trapped Ion Mobility Spectrometry

Cameron N. Naylor,[1] Tobias Reinecke,[1] Mark E. Ridgeway,[2] Melvin A. Park,[2] Brian H. Clowers[1] (iD)

[1]Department of Chemistry, Washington State University, Pullman, WA 99164, USA
[2]Bruker Daltonics Inc., Billerica, MA 01821, USA

Abstract. Using contemporary theory for ion mobility spectrometry (IMS), gas-phase ion mobilities within a trapped ion mobility-mass spectrometer (TIMS) are not easily deduced using first principle equations due to non-linear pressure changes and consequently variations in E/N. It is for this reason that prior literature values have traditionally been used for TIMS calibration. Additionally, given that verified mobility standards currently do not exist and the that the exact conditions used to measure reported literature values may not always represent the environment within the TIMS, a direct approach to validating the behavior of the TIMS system is warranted. A calibration procedure is presented where an ambient pressure, ambient temperature, two-gate, printed circuit board drift-tube IMS (PCBIMS) is coupled to the front of a TIMS allowing reduced mobilities to be directly measured on the same instrument as the TIMS. These measured mobilities were used to evaluate the TIMS calibration procedure which correlates reduced mobility and TIMS elution voltages with literature values. When using the measured PCBIMS-reduced mobilities of tetraalkyl ammonium salts and tune mix for TIMS calibration of the alkyltrimethyl ammonium salts, the percent error is less than 1% as compared with using the reported literature K_0 values where the percent error approaches 5%. This method provides a way to obtain accurate reference mobilities for ion mobility techniques that require a calibration step (i.e., TIMS and TWAVE).

Keywords: Trapped ion mobility spectrometry, Drift-tube ion mobility spectrometry, Ion mobility calibration, Mass spectrometry

Introduction

For experiments using drift-tube ion mobility spectrometry (DT-IMS), the rate of ion migration through an electric field is dependent upon the nature of the target ion and a neutral gas. Though ion drift velocity is the parameter measured in a DT-IMS, this quantity can be related to gas-phase ion mobility parameter and to an ion-neutral collisional cross section (CCS)

Correspondence to: Brian Clowers; e-mail: brian.clowers@wsu.edu

through a number of assumptions [1]. Factors that impact mobilities include pressure, temperature, and the electric field strength. To account for different pressures and temperatures among different instrumental configurations, mobilities are commonly normalized, through a first approximation, for pressure and temperature to yield a reduced mobility value (Eq. (1)) [1–6].

$$K_0 = \frac{l^2}{U*t_d} \frac{P}{P_0} \frac{T_0}{T} \qquad (1)$$

Here, l is the length of the drift tube in centimeters, U is the applied voltage, t_d is the drift time of the ion in seconds, P is the

pressure in Torr, T is the temperature in Kelvin, and P_0 and T_0 are 760 Torr and 273 K respectively to normalize for pressure and temperature. Reduced mobilities may be calculated directly from the measured drift time using Eq. (1) or from the slope of an arrival time distribution for different drift voltages which plots observed drift times against pressure over voltage [7]. The reduced mobilities of ions provide valuable analytical information with applications spanning from chemical warfare agent detection to proteomics [8–11].

Within recent years, a new type of IMS has been developed, trapped ion mobility spectrometry (TIMS) [12–15]. As opposed to the counter-current flow of neutral drift gas in a DT-IMS system, ions within a TIMS system interact with buffer gas that is moving in the same direction as the ions while they are retarded by a dc field and radially confined by an rf field within the tunnel. This trapping configuration induces a mobility-driven spatial stratification based on size and charge, with larger species (i.e., low mobility) collecting towards the exit of the tunnel and smaller species near the entrance. To scan ion populations into the MS, the dc field within the tunnel begins to ramp reducing the depth of the potential well allowing ions to elute from the end of the tunnel [12, 14–18]. As opposed to DT-IMS which is a time dispersive technique, the TIMS is an ion-trapping approach. Another key difference between the two approaches is that for DT-IMS systems, the higher mobility species (i.e., smaller) arrive at the detector first, whereas in TIMS, the lower mobility species (i.e., larger) are the first to exit the system.

TIMS offers many advantages compared with traditional drift-tube IMS. In the commercial TIMS-TOF, which includes a two-stage TIMS configuration, ions are continuously collected in the front of the TIMS tunnel before being pulsed into the latter section of the TIMS tunnel for mobility separation. This method, known as parallel-accumulation serial fragmentation (PASEF), allows for a nearly 100% duty cycle [19] and has a wide range of applications including global proteomics and complex sample analysis [20]. A single-stage TIMS, as featured in the present work, does not allow for parallel accumulation, however, incorporates a range of functionality that finds applications across disciplines [15, 21–24]. Separation capacity is one such benefit where applying a small voltage gradient across the TIMS tunnel for an extended length of time lends to high-resolution separation of species such as different ubiquitin, bradykinin, and substance P configurations in the collisional cross-section domain [15, 24]. Another trait that differentiates TIMS from DT-IMS is the ability to trap ions for an extended time allowing reactions to occur in the gas phase prior to separation. One recent application used TIMS to analyze the decomposition of explosives as they are trapped for varying lengths of time [21]. However, since the electric field is dynamic and the exact temperature within the TIMS tunnel is not known (but is assumed to be close to room temperature), reduced mobility and collisional cross-section values cannot be directly calculated and must be indirectly determined by calibrating the TIMS with standards that have K_0 values reported in the literature.

Currently, there are three reported methods for calibrating a TIMS. Hernandez et al. present a method which graphs inverse reduced mobility versus the experimental elution voltage. In this approach, the time spent outside of the TIMS device is calculated to find the elution voltage and a subsequent plot is constructed where the y intercept is the voltage applied to the exit funnel and the slope is called the "A-term." This last calibration plot is applicable for all experiments performed at those TIMS settings [14]. Michelmann et al. presented another method where inverse elution voltage is graphed against literature-reduced mobility. The advantage of this method is that the calibration equation directly allows for the K_0 of an unknown compound to be found from the best-fit equation [16]. In both previous methods, elution voltage is inversely related to reduced mobility and dependent on the voltage applied to the exit funnel. In the most recent method reported by Chai et al., the TIMS calibration is modeled by a Taylor expansion series derived from a Boltzmann transport equation [25]. The benefit of this method is it is sample independent, yet the model is still developed using reference K_0 values reported by Stow [26] and compared with the previous calibration procedure reported by Michelmann [16, 25]. This dependence is also true for the methods by Michelmann et al. and Hernandez et al. which rely on literature K_0 values for the standards that are used to calibrate the TIMS. Even though reduced mobility normalizes for temperature, reported K_0 values differ as a function of temperature [5, 27–29], and literature K_0 values for the same species may differ significantly from each other even for stable (i.e., non-conformation changing) compounds in the gas phase. For example, reported K_0 values for tetrabutylammonium range from 1.39 to 1.28 cm^2 V^{-1} s^{-1} depending on the reference and the reported conditions (or lack thereof) under which the measurements were taken [30–33]. With such a wide range of mobility values for one ion species where experimental conditions may not be reported, precision for TIMS calibration might be high with an $R^2 > 0.999$ if all the values are used from the same reference [14, 16], but accuracy is relative to the single reference of literature K_0 values used. Therefore, with the variation among literature values, the challenge becomes finding reported K_0 values that were recorded under conditions that are suitable for TIMS calibration.

One strategy for calibration might be using an alternative calibrant, such as polyethylene glycol as Haler et al. proposes [34], which also comes with a range of assumptions, such as the molecules remain in constant shape, and therefore collisional cross section, at all effective temperatures. This thermometer ion-like behavior may not qualify polyethylene glycol and other synthetic polymers as a suitable mobility standard for calibration [25, 35, 36]. If a TIMS is tuned for a lower mass range, a full mobility calibration using a series of hexa-substituted oxyphosphazenes, colloquially known as tune mix [14, 16, 25], is not possible due to the wide mass and mobility range of the compounds in that solution. Thus, lower mass standards are needed for a TIMS tuned for high mobility. However, low mass/high mobility standards are usually used

on higher temperature and pressure IMS systems with a drastically different experimental environment than the conditions within the TIMS cell [5, 37, 38].

Here, we present a method for calibrating a TIMS that does not rely on literature values for mobility standards but uses the experimentally deduced mobilities from a drift-tube system coupled directly to the TIMS-TOF system. A printed circuit board ion mobility spectrometer (PCBIMS) is attached to the endplate and transfer capillary inlet of the TIMS device (Figure 1). The PCBIMS is operated at ambient pressure where ionization occurs and at room temperature in an attempt to mimic the conditions within the TIMS. In addition, the PCBIMS attached to the TIMS allows for any instrument-specific biases to be accounted for when measuring mobility. Specifically, three series of low mass standards for calibration, tune mix, tetraalkyl ammonium salts (TXA), and alkyltrimethyl ammonium salts (XTMA), and report the mobilities of each. Furthermore, the findings are verified with reduced mobility values of three different stand-alone IMS systems.

The merit of this proposed method is the accessibility of the open-source PCBIMS design, which allows this approach to be easily implemented by other research groups using TIMS system or TWAVE systems that require external calibration [39]. Lowering barriers to direct calibration under laboratory-specific conditions allows researchers to conduct experiments using the higher sensitivity configuration of the instrument (i.e., not with the high-pressure drift cell attached) with higher degrees of confidence and use of calibration values that may not exist in the open literature. Finally, this approach allows for DT-IMS data and TIMS data to be collected sequentially without needing to change the setup.

Experimental

Sample Preparation　The following TXA and XTMA salts were purchased from Sigma-Aldrich (St. Louis, MO) for use as mobility calibrants: tetrapropyl ammonium bromide (Sigma: 225568-100G) (T3A), tetrabutyl ammonium bromide (Sigma: 426288-25G) (T4A), tetrapentyl ammonium bromide (Sigma: 241970-25G) (T5A), tetrahexyl ammonium bromide (Sigma: 252816-25G) (T6A), tetraheptyl ammonium bromide (Sigma: 87301-10G) (T7A), tetraoctyl ammonium bromide (Sigma: 294136-5G) (T8A), tetrakis-decyl ammonium bromide (Sigma: 87580-10G) (T10A), tetradodecyl ammonium bromide (Sigma: 87249-5G) (T12A), decyltrimethylammonium bromide (Sigma: 30725-10G) (10TMA), dodecyltrimethylammonium chloride (Sigma: 17104-25G) (12TMA), trimethyl-tetradecylammonium chloride (Sigma: 87212-5G) (14TMA), trimethyloctadecylammonium bromide (Sigma: 359246-10G) (18TMA), and benzyltriethylammonium chloride (Sigma: 146552-25G) (phen-TEA). Tune mix (Agilent Part Number: G2431A/G2431-60001, Agilent, Santa Clara, CA) consisted of a mixture of hexamethoxyphosphazene, hexakis(2,2-difluoroethoxy)phosphazene, hexakis(1H,1H,3H-

tetrafluoropropoxy)phosphazene, hexakis(1H,1H,5H-octafluoropentoxy)phosphazene,

hexakis(1H,1H,7H-dodecafluoroheptoxy)phosphazene, hexakis(1H,1H,9H-perfluorononyloxy)phosphazene, Tris(heptafluoropropyl)-s-triazine, betaine, and trifluoroacetic acid, ammonium salt in a mixture of 31:2 acetonitrile and water.

The calibration standards for mobility values using tune mix were diluted in a 1:10 ratio, 800 nM for TXA salts (T3A-T12A), and 800 nM for XTMA salts (10TMA-18TMA, Phen-TEA) in acetonitrile (Optima LC/MS grade, Fisher Chemical, Fair Lawn, NJ). The concentrated TXA calibration standard used for Faraday plate data experiments consisted of a 100 μM T5A-T12A in methanol (HPLC grade, Fisher Chemical, Fair Lawn, NJ). Literature mobilities, if available, and *m/z* values for these standards are presented in Table 1.

Instrumentation　A prototype TIMS funnel (Bruker Daltonics, Billerica MA) was incorporated into a micrOTOF-Q III ESI-QqTOF mass spectrometer (Bruker Daltonics, Billerica MA) within the first vacuum stage. Two roughing pumps, a SOGEVAC 40BI (Leybold USA Inc., Export, PA) and Edwards 28 (Edwards, Sanborn, NY), were used for the micrOTOF-Q-III. A higher frequency (1147.5 kHz) rf card was used in the micrOTOF-Q-III to allow for a lower mass cutoff for high mobility ions. Ions were directed into the TIMS entrance funnel from the deflector which had one set voltage applied to "turn on" which allows for filling of the trap. After a specified time has elapsed, the deflector changes to another voltage applied to "turn off" where the trap does not fill and allows for ions within the TIMS tunnel to separate (Figure 2). As noted elsewhere [12, 14, 15], the TIMS was constructed using printed circuit boards (FR-4) with three main regions: the entrance funnel, the TIMS tunnel, and the exit funnel. To facilitate transport ions exiting the TIMS tunnel, a constant potential was applied to the entrance and exit funnels. As illustrated in Figure 2, the potentials in the TIMS tunnel can be adjusted such that the voltage gradient ramps throughout the experiment. The TIMS can be operated in two modes: "transmission mode" or in ramping mode to obtain a mobility separation. In transmission mode, the dc potentials applied to each region gradually decrease to guide ions into the TOF for analysis. For TIMS analysis, ions are trapped within the TIMS tunnel radially confined by an rf field to prevent diffusion and the dc ramped in order to gradually elute ions of different mobility and thus to provide ion mobility separation from collisions with the carrier gas.

The printed circuit board IMS (PCBIMS) was constructed according to the procedure noted elsewhere [40]. Briefly, the PCBIMS used two tri-grid shutter gates described by Langejuergen et al. [41, 42] rather than a Bradbury-Nielsen gate for simplicity. The gates were driven by FET pulsers described by Garcia et al. [43], which were controlled by a waveform generator (*Analog Discovery 2*,
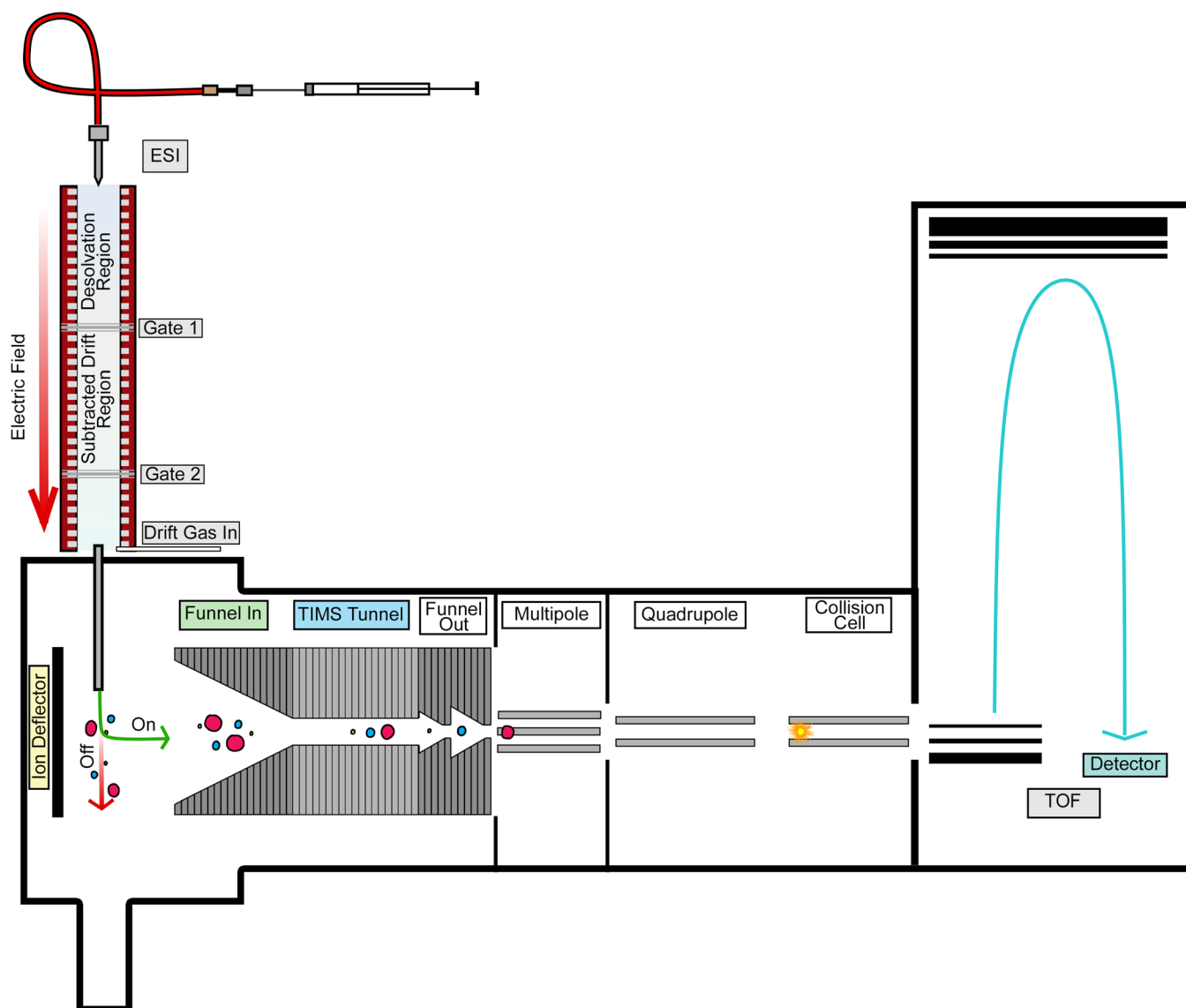
Figure 1. Diagram of PCBIMS-TIMS. The PCBIMS is directly attached to the transfer capillary where the Apollo II ESI was attached. For PCBIMS spectra, the TIMS is operated in transmission mode and one of the two tri-grid shutter gates on the PCBIMS is pulsed (Figure 4). For TIMS calibration, both PCBIMS gates remain open and the TIMS is operated normally.

Digilent Inc., *USA*). The DT-IMS system had the following dimensions: the length of desolvation region was 10.4 cm, the drift region between the gates 1 and 2 was 10.4 cm, the region after the second gate before the capillary was 3.4 cm, and the region between the last electrode and the end plate on the micrOTOF-Q-III was 4 mm. The sides of the PCBIMS were sealed using Torr Seal (Agilent, Santa Clara, CA) to attach plates to the sides of the drift tube to ensure no excess gas or water vapor entered the drift tube. Voltages were measured at gates 1 and 2 with a Fluke 8846A Precision Multimeter (Omega, Everett, WA) and high voltage probe. Voltages were corrected for the impact of the voltage probe on the measurement as described by Hauck et al. [44]. Briefly, voltages were measured at each gate with a high voltage probe, and the reading from the multimeter is corrected for the electrical series that was

created when the probe was applied to the gate since a small amount of the current was directed through the multimeter rather than the IMS [44]. A thermocouple was inserted in the endplate to ensure the capillary within the micrOTOF-Q-III was at room temperature and matched the ambient temperature reading in the lab. Ambient pressures and temperatures were measured using an Omega OM-CP-PRHTEMP2000 (Omega Engineering Inc., Norwalk, CT) placed next to the drift tube. Nitrogen was injected into the back of the drift tube after the last electrode from the same liquid nitrogen tank that was used for the rest of the micrOTOF-Q-III at a flow rate of $1.0 \text{ L} \times \text{min}^{-1}$ set through the OTOF software (Bruker Daltonics, Billerica MA). All data was extracted using PNNL UIMF Viewer and processing was performed in Igor 7 Pro (Wavemetrics, Lake Oswego, OR).

Table 1. The Three Classes of Standards Used in this Study (TXA, XTMA, and Tune Mix) Are Listed Alongside the Observed m/z for the Species, the K_0 Values Found in Literature if Present, the K_0 Value from the Arrival Time Distribution Plots, the K_0 from Setting the Arrival Time Distribution Plot Through 0, and the Directly Calculated K_0 Using Eq. (1). The Last Column is the K_0 Values for the TXA Salts from Another Instrument Within Our Laboratory

	m/z	Literature [26, 33] K_0 (cm^2 V^{-1} s^{-1})	Arrival time Dist K_0 (cm^2 V^{-1} s^{-1})	Arrival time Dist (set Y_0 to 0) K_0 (cm^2 V^{-1} s^{-1})	Direct calculation K_0 (cm^2 V^{-1} s^{-1})	Literature-direct Cal. K_0	Davis K_0 values [51, 52] (cm^2 V^{-1} s^{-1})
T3A	186	1.506	1.445	1.443	1.444 ± 0.008	− 0.063	1.478
T4A	242	1.28	1.239	1.235	1.236 ± 0.008	− 0.045	1.257
T5A	298	1.116	1.077	1.072	1.073 ± 0.007	− 0.044	1.085
T6A	354	0.986	0.948	0.947	0.948 ± 0.007	− 0.039	0.956
T7A	410	0.883	0.847	0.853	0.855 ± 0.005	− 0.03	0.859
T8A	466	0.808	0.778	0.781	0.782 ± 0.005	− 0.027	0.783
T10A	578	0.702	0.678	0.68	0.681 ± 0.005	− 0.022	0.673
T12A	690	0.644	0.608	0.618	0.620 ± 0.004	− 0.026	0.602
10TMA	200		1.270	1.265	1.265 ± 0.002		
12TMA	228		1.155	1.167	1.168 ± 0.004		
14TMA	256		1.070	1.095	1.097 ± 0.007		
18TMA	312		0.997	1.006	1.007 ± 0.004		
Phen-TEA	192		1.442	1.465	1.466 ± 0.007		
TM322	322	1.371	1.345	1.330	1.330 ± 0.007	− 0.046	
TM622	622	1.018	0.957	0.975	0.98 ± 0.01	− 0.033	
TM922	922	0.842	0.777	0.794	0.797 ± 0.007	− 0.038	
TM1522	1522	0.644	0.572	0.596	0.597 ± 0.006	− 0.041	

Results and Discussion

Drift-Tube IMS Measurements

To provide a frame of reference for IMS performance of the system before coupling to the TIMS, reference K_0 values were determined using a stand-alone PCBIMS with a Faraday plate detector [40]. The standard DT-IMS metrics such as resolving power and reduced mobility values determined from first principles were measured for the target calibrant species. A Faraday plate and aperture grid were attached to the back of the PCBIMS described above. In this configuration, the drift length between the first gate and Faraday plate was determined to be 14.5 cm. Only the first gate was pulsed with a gate pulse width of 479 μs and each measurement consisted of a total of 1000 averaged spectra.

To gain a reference set of K_0 values for the TXA salts, a 100 μM solution of T5-T12A was used. The electric field was varied systematically to create an arrival time distribution plot. Subsequently, K_0 values were directly calculated from the arrival time distribution shown in Figure 3 and are reported in Table 2. In the case of all TXA salts, the y intercept was 0 within the error of the fit with the linearity of $R^2 > 0.9997$ for each species. The y intercept indicates the ions were not spending any excess time between the last electrode and Faraday plate. Using a similar instrument, it is possible to attain higher resolving powers approaching 100 with a lower gate pulse width [45]. However, in the interest of expediting the experimental campaign, a larger gate pulse width was used to maximize ion throughput and consequently the signal to noise ratio. For this configuration, the resolving power for the TXA salts in this system ranged from 65 to 79 with an overall average of 72 ± 5 (Table 2, Supplemental Figure 1). As a stand-alone system, these K_0 values and resolving powers are reasonable for the PCBIMS and will be used for comparison for the two studies described below.

Dual-Gate PCBIMS-TIMS

For the next experiments, the Faraday plate and aperture grid were removed, and the PCBIMS was attached to the transfer capillary inlet on the TIMS-micrOTOF-Q-III. In general, the dual-gate PCBIMS can be operated in one of three ways using the two-gate system: scanning mode [46], Fourier transform mode [47], or the two-gate subtraction method [48]. Scanning mode involves both gates being pulsed and will only allow for a select range of mobilities to enter the TIMS at one time. To gain a full mobility spectrum, the time delay between pulsing the first and the second gate is slowly increased with each experiment [46]. The scanning method ensures the accuracy of knowing what range of mobilities enters the TIMS and grants a direct connection to the elution voltage. However, this method requires that the operator knows the mobilities of the ions of interest and picks the range that accommodates those ions to avoid scanning over the complete mobility range resulting in prolonged analysis times [46].

The second option is Fourier transform, where the voltages applied to the gates are swept over a length of time [47]. However, the longest TIMS experiment allowed by the build on our system is a 2 s TIMS scan, and an FT spectrum with sufficient statistical signal would require longer than that to acquire. To avoid changes to the TIMS software and ensuring the PCBIMS coupling method is easily implemented by other users, this method was not chosen.

The third method, and ultimately the one chosen for the calibration of the TIMS described below, is the gate subtraction method similar to what is described by Hauck et al. to ensure accurate mobility values from a dual-gate DT-IMS [48, 49]. For a two-gate IMS system, an experiment is performed twice: the first experiment with gate 1 pulsed and gate 2 constantly open, and the second experiment with gate 1 constantly open and gate 2 pulsed. From these data, the drift times from gate 2
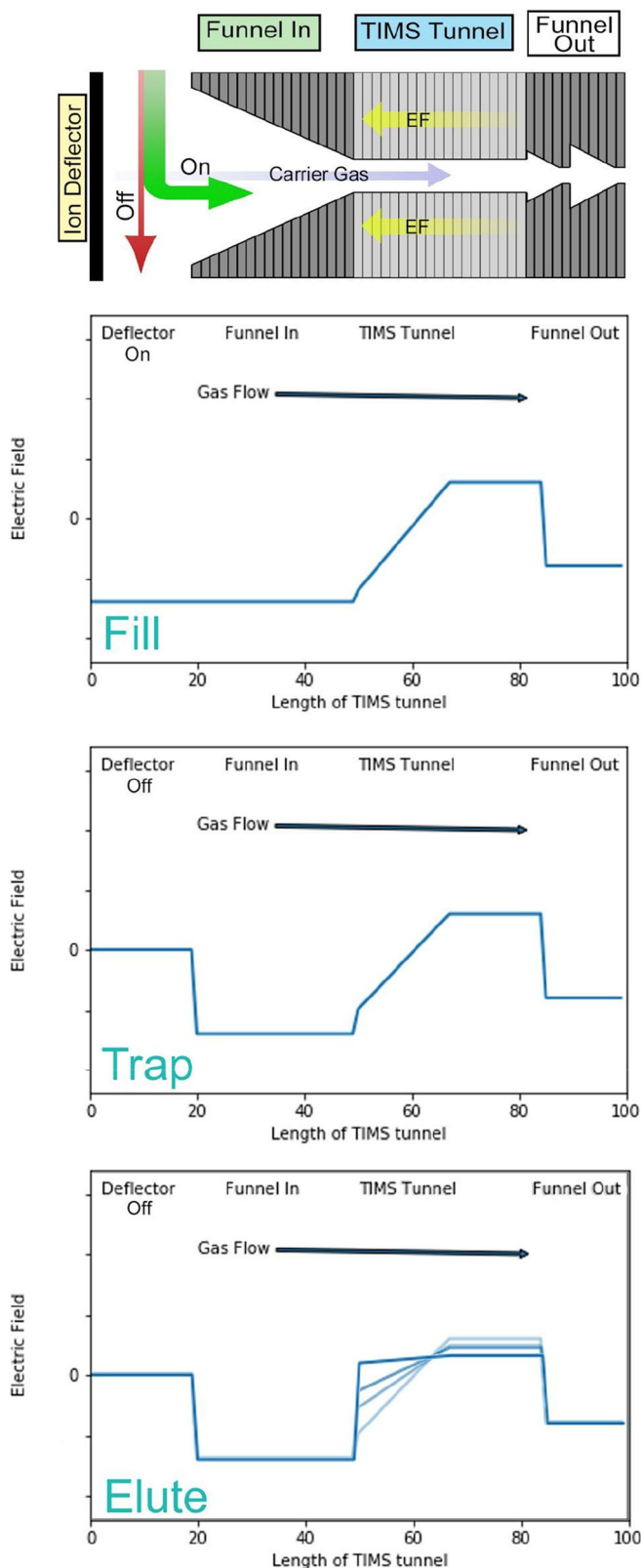
Figure 2. How the TIMS scan is operated: the TIMS first has the open deflector to allow ions into the funnels. The ions are then trapped once the deflector turns off, and elute as the voltages in the TIMS tunnel start to ramp

can be subtracted from the drift times from gate 1 (Figure 4). This difference in drift time between the two gates gives an altered arrival time distribution since subtracting the drift time from gate 2 also removes the excess time spent outside the drift cell, such as time spent in the TOF or traveling through the TIMS cell, from the spectra. K_0 values can be obtained from the slope of an arrival time distribution plot of these subtracted drift times by varying the electric field. Due to the differential measurement, y intercept from the arrival time distribution plot (the y_0 value) should be close to 0 ms within error, similar to Faraday plate data from a single gate system. Alternatively, two arrival time distribution plots can also be made for both experiments pulsing each gate and subtracting out the slopes and y intercepts will yield the same results as just subtracting the drift times. K_0 values can also be directly calculated from each experiment since the pressures, temperatures, and voltages are recorded for each experiment. Directly calculating the K_0 values proves to be more accurate since there is a mild dependence of K_0 values on the electric field, which would add error to an arrival time distribution plot [44]. Ultimately, the gate subtraction method was chosen for the efficiency of the experiments, simplicity of theory and application for coupling to the TIMS, and the ability to accurately calculate K_0 values directly from a few parameters.

For this set of experiments, the voltages were varied systematically and used a gate pulse width of 0.95 ms, which was needed to ensure a sufficient number of ions survive the transfer from atmospheric to reduced pressure. Since the TIMS deflector was what ultimately triggered the gate of choice on the PCBIMS, the open deflector voltage was set slightly higher (200 V) than closed deflector voltage (120 V), but both were higher voltages than the entrance funnel (70 V), leading to a continuous ion transfer into the TIMS tunnel. The TIMS was held in "transmission mode" while mobilities were measured from the PCBIMS, ensuring that the only mobility data was from the PCBIMS. The TIMS was set to collect for 100 accumulations per LC frame for 50 LC frames for a total of 5000 averaged spectra.

When determining the mobilities of the different ion populations using the two-gate subtraction method combined with the TOF-MS system, we observed that y_0 value was not always zero within the error of the fit. While an intercept of zero was consistently observed for higher mobility species, some of the larger calibrants (Supplemental Figures 2 and 3) such as tune mix m/z of 622 and 922, T12A, and TM18A exhibited non-zero y intercepts (mobilities from the slopes of these plots are shown in Table 1). Compared with the absolute drift times of the ions across the drift region (i.e., between the two gates), the observed deviation from an ideal intercept for these larger ions is attributed to the necessity of extrapolating fits to experimental data points that correspond to arrival times of 10's of milliseconds to an intercept close to zero. Stated differently, the expansion of the confidence bands surrounding the fit to the data points, by definition, expands as the distance from the data
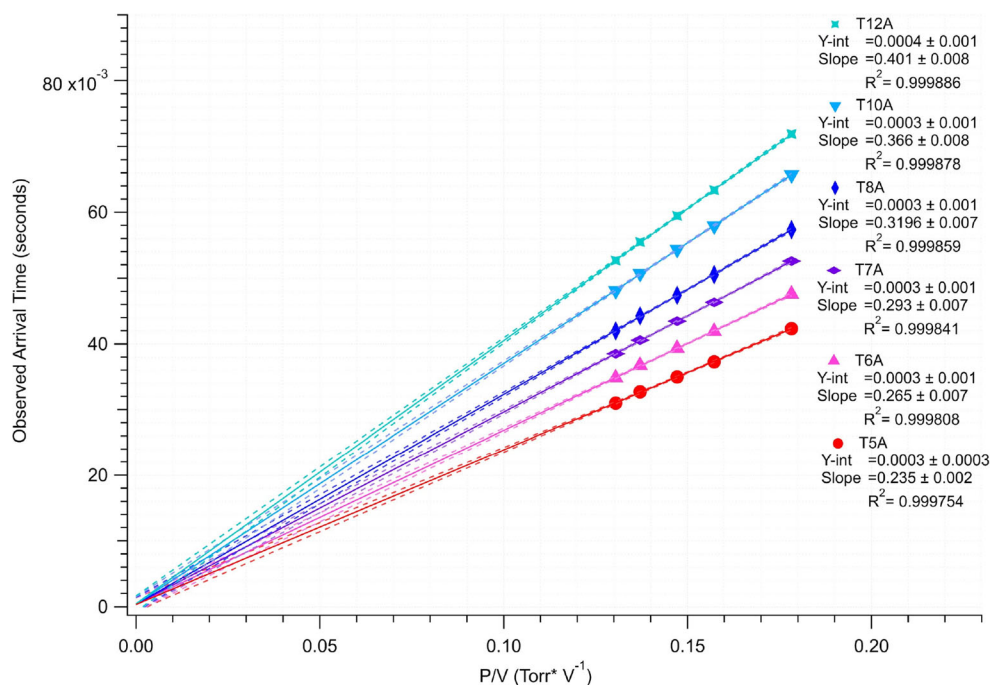
Figure 3. Arrival time distribution of the TXA salts using the Faraday plate as a detector. All y intercepts are 0 within error and each of the fits are highly linear. The K_0 values from the slopes are reported in Table 3

range increases. Because the two-gate method is predicated on a well-defined drift region, the subsequent experimental values for calibration were derived from fits where the y intercept is forced through 0. The K_0 values calculated from the resulting slopes using this method are summarized in Table 1. Close examination of Table 1 illustrates that the K_0 values calculated by fitting the y intercept of the arrival time distribution through 0 are statistically the same as those K_0 values that were directly calculated from each electric field measurement using first principles assumptions. These statistically similar K_0 values suggest that the first principles approach or slope determination by force fitting the intercept through 0 are the preferred methods for calibration when using the two-gate subtraction method. For systems where the observed arrival times are closer to zero force fitting, the intercept may not be necessary.

Also presented in Table 1 are the literature values reported for the tetraalkyl ammonium salts [33] and tune mix [26] as

Table 2. K_0 Values from the Arrival Time Distribution Slopes and the Directly Calculated K_0 Values from the Drift Times from the Faraday Plate Data. These K_0 Values Are Closer to the K_0 Values Reported in Table 1 than the Literature Values also Reported in Table 1. In Addition, the Experimental Resolving Power of Each Salt Is Reported in the Last Column

	Arrival time Dist K_0 (cm^2 V^{-1} s^{-1})	Direct calculation K_0 (cm^2 V^{-1} s^{-1})	Experimental R_p
T5A	1.077	1.061 ± 0.003	65 ± 2
T6A	0.958	0.944 ± 0.002	68 ± 1
T7A	0.866	0.855 ± 0.002	71 ± 2
T8A	0.794	0.784 ± 0.002	74 ± 4
T10A	0.692	0.685 ± 0.001	77 ± 6
T12A	0.633	0.626 ± 0.001	79 ± 7

measured on the Agilent 6560. The difference between these values and the directly calculated K_0 values are in Table 1 illustrating there is an offset between the literature values and the experimentally determined values. In addition to the fact that not all of the experimental conditions are known for the Agilent 6560 and if those conditions are directly analogous to the conditions within the TIMS, one possible cause of the discrepancy is that for all experimental parameters reported in the literature, the back ion funnel after the drift region in the Agilent 6560 was kept at a constant voltage [26] and not varied with the electric field within the drift region [50]. Since there is no gate separating the two regions in this instrument, the inhomogeneous electric field may cause an offset in K_0 values while maintaining precision [50]. In addition, the exit funnel in the TIMS is considered to affect the elution voltages of the ions, to such a degree that the voltage is a variable (the y intercept in the A-term plots) [14] in the calibration equations. As a result, an offset in K_0 values will cause an offset in TIMS calibration and creates a significant impact on the mobilities of unknown compounds found from the calibration curve [14, 16]. One additional factor for the difference in these K_0 values reported from the Agilent 6560 is the number density. According to the settings reported by Stow et al., the E/N for their experiment is 12.5 Td, which puts their mobilities nearing the mid-field region [26]. For the experiments conducted on the PCBIMS-TIMS, the E/N varied from 0.8 to 1.8 Td (Supplemental Table 1), which is more analogous to TIMS conditions since TIMS is considered to be a "soft" mobility technique [15, 24]. The last factor that lends uncertainty to the reference K_0 values is the length of drift tube used for the calculations reported by Stow et al. is an average against a "reference
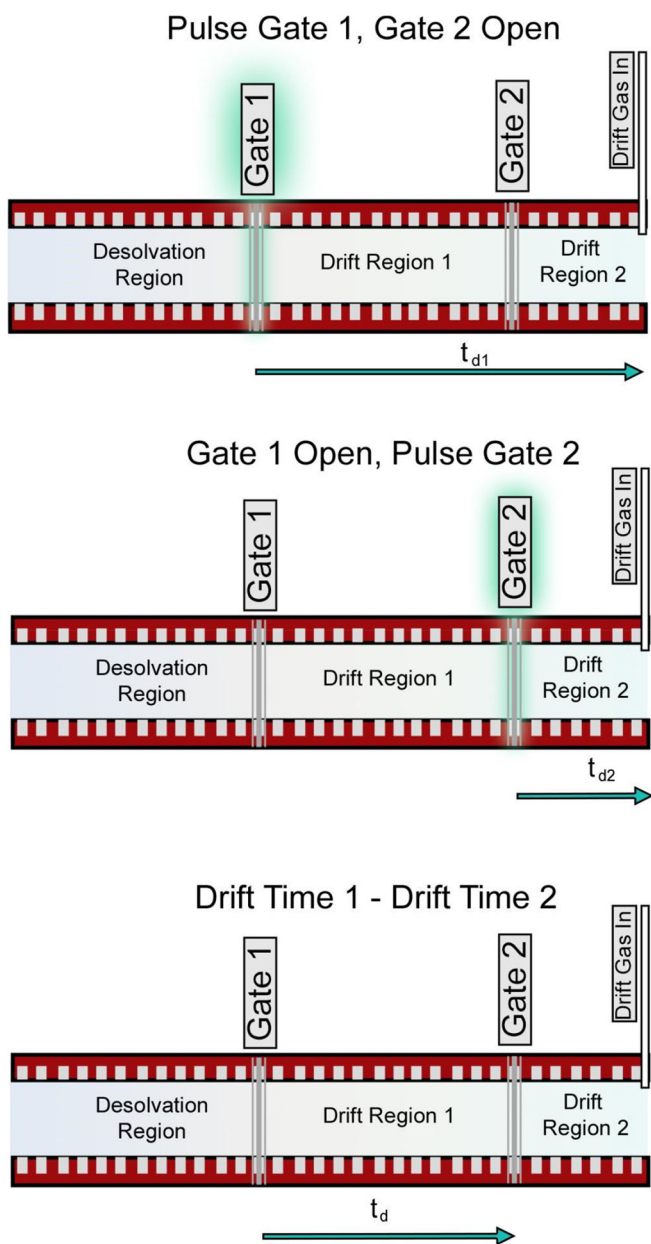
Figure 4. The gate subtraction method of operating the PCBIMS: by subtracting the drift time after the second gate (t_{d2}) from the drift time of the first gate (t_{d1}), the subtracted drift time (t_d) is void of the time spent outside of the IMS device and since the distance between the gates is accurately known, the K_0 value for the subtracted drift time is accurate

system," and is not the lengths of each individual drift tube used in the study [26]. This average of all 4 drift tubes would explain the precision of the resulting mobilities, but would not be accurate since the actual lengths of each drift tube was not used.

The K_0 values using the PCBIMS-TIMS presented in Table 1 are closer to the K_0 values calculated from the Faraday plate data of the PCBIMS than the literature values presented, suggesting that coupling to the TIMS and using the gate subtraction method did not deteriorate the performance of the

instrument. In addition, all the K_0 values presented here from the PCBIMS are in close agreement with other K_0 values for the tetraalkyl ammonium salts (Table 1) determined via sweeping different electric fields on a separate instrument as described by Davis et al. [51, 52] and determined via frequency modulating and sweeping the voltage on another separate instrument [53] which lends confidence to our K_0 values.
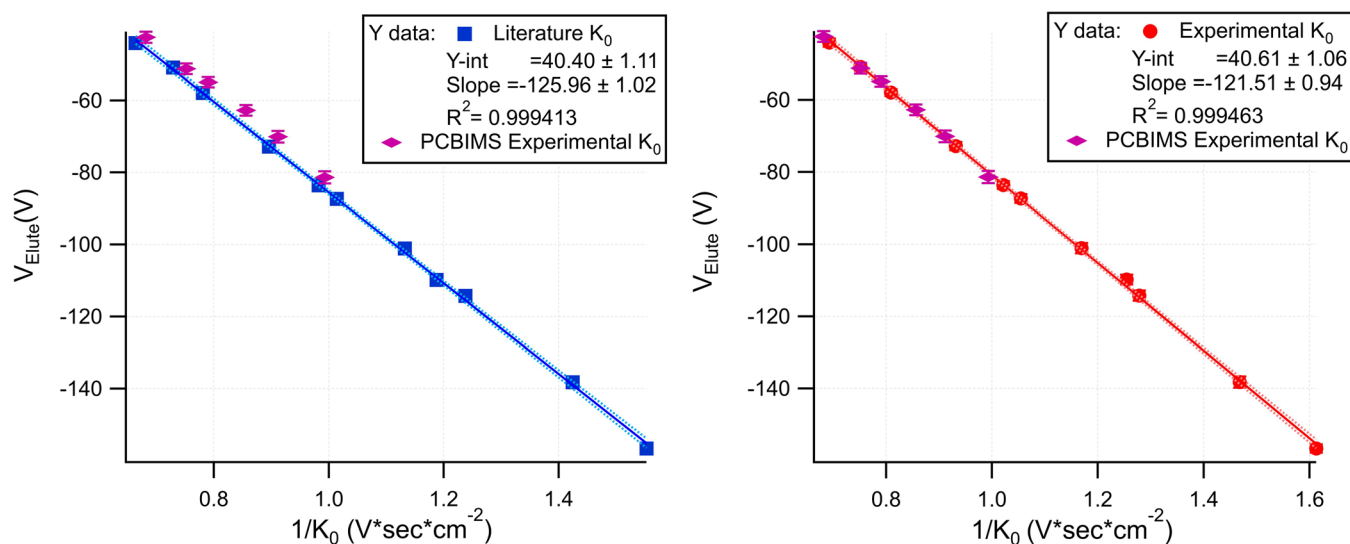
TIMS Calibration

For TIMS only experiments, there are two options to introduce ions into the TIMS for analysis: either the PCBIMS is set to have both gates open and the highest electric field or the original Apollo ESI source from the micrOTOF-Q-III is reattached. The TIMS was calibrated according to the method developed by Hernandez et al. [14] and Michelmann et al. [16] for TIMS ramps suited to capturing all mobilities in the calibration standards at a pressure of 1.88 Torr (2.5 mBar), using the values obtained from the PCBIMS as the reference K_0 values. The TIMS was set to collect for 100 accumulations per LC frame for 20 LC frames for a total of 2000 averaged spectra. Details for TIMS experimental settings are contained in Table 2 in the Supplemental Material.

TIMS calibration plots using both the PCBIMS direct calculation K_0 values and the literature values are presented in Figure 5. The plots described by Hernandez et al. [14] were used because the y intercept should correspond to the experimental voltage applied to the exit funnel. In both graphs, there is little difference between the y intercepts and the R^2 value, illustrating that both methods are equally precise. However, the slopes of these plots differ enough that the K_0 value is affected, especially for lower mobility ions, which are farther away from the y intercept.

Since precision of both calibration plots created from the literature and experimental K_0 values respectively had been addressed to test the accuracy of each calibration using the experimental and literature K_0 values, the alkyltrimethyl ammonium salts were withheld from the initial construction of the TIMS calibration curve. Using the same TIMS parameters for the calibration curves consisting of the tune mix and tetraalkyl ammonium salts, the alkyltrimethyl ammonium salts were measured under the same conditions. Using the resulting calibration equation for both calibration graphs, using literature and experimental K_0 values, K_0 values were calculated for the alkyltrimethyl ammonium salts, and the calibration curve K_0 values can be compared with those from the experimental PCBIMS K_0 values that were previously determined (Table 3). Additionally, the TIMS elution voltages for the alkyltrimethyl ammonium salts are superimposed on both calibration curves (the pink diamonds) in Figure 5 using the experimental K_0 values from the PCBIMS calibration. The data overlay the calibration line within error using the K_0 values generated from the PCBIMS. However, for the graph where the literature K_0 values are used for the TIMS calibration, there is an offset from the experimental alkyltrimethyl ammonium salts values. The percent errors for the XTMA salts K_0 values from

Figure 5. TIMS calibration of the TXA salts and tune mix using the literature values [26, 33] (blue squares), and the experimental values from the PCBIMS (red circles). The XTMA salts were withheld from the calibration and are plotted on both graphs with their TIMS elution voltage and the experimental K_0 values from the PCBIMS values. When the literature values are used for TIMS calibration, there is an offset with the XTMA salts

both calibration curves are presented in Table 3. Using the PCBIMS K_0 values for TIMS calibration, the error is a maximum 1% whereas if the literature values were used, the error is approaching 5%. Combined with the consistent K_0 values for the TXA salts presented in the previous two sections and the small percent error of the XTMA salts from TIMS calibration, using the PCBIMS to obtain K_0 values does not change the precision of the calibration process but improves the accuracy of the TIMS calibration curve.

Conclusions

Through the present effort, we have demonstrated the coupling of a high-performance, open-source, cost-effective, dual-gate drift-tube system to a TIMS-micrOTOF-Q-III as a means to validate the calibration of the TIMS system using the relevant conditions. The PCBIMS has demonstrated consistent K_0 values measured both in Faraday mode and coupled to the TIMS with less than 1% variance and those K_0 values are close to the K_0 values for the tetraalkyl ammonium salts measured on three different instruments within our laboratory. When those

K_0 values are used to calibrate the TIMS, the resulting calibration curve gives a maximum of 1% error from the experimental K_0 values measured on the PCBIMS alone, as compared with only using literature values which yields an error of 5%. The coupling of the PCBIMS to the TIMS systems allows for mobilities to be directly measured on a single platform which normalizes for differences that historically arise between the system under test (i.e., the TIMS) and the conditions under which the literature values were obtained (i.e., the external drift cell generating literature values). In addition, the coupling of the open-source PCBIMS no longer confines TIMS calibration to literature K_0 values and any mobility standard of choice can be used. TIMS calibration can now be custom tailored to the analyte of interest instead of using a single calibration set which encompasses a wide mass/mobility range and not necessarily reflect the chemical nature of the target analytes. To be clear, the use of the PCBIMS system serves a secondary validation step and establishes a foundation to build upon the high-resolution capabilities of the TIMS platform. More accurate calibration of a variety of different K_0 values will benefit future TIMS research for a broad range of applications, especially in the low mass/high-mobility domain. Using this approach

Table 3. For a TIMS Ramp of − 170 to 20 V with Funnel 1 Out at 36 V, the Elution Voltages for the XTMA Salts and Tune Mix m/z 322 Are Presented. The Second Column is the Experimental K_0 Value from the PCBIMS and the two Following Columns are the Calculated K_0 Values from the Calibration Curves Generated from TIMS Calibration with the PCBIMS and Literature K_0 Values for the Tune Mix and TXA Salts Respectively (from Figure 5). Treating the PCBIMS Experimental K_0 Values as the Actual Values, the Percent Error for both TIMS Calibration K_0 Values Is in the Last Two Columns

	V_{elute} (V)	PCBIMS K_0 (cm^2 V^{-1} s^{-1})	TIMS Lit K_0 (cm^2 V^{-1} s^{-1})	TIMS Exp K_0 (cm^2 V^{-1} s^{-1})	TIMS Lit % error	TIMS Exp % error
10TMA	− 54.9 ± 1.4	1.265	1.321	1.272	4.444	0.535
12TMA	− 62.8 ± 1.5	1.168	1.221	1.175	4.515	0.62
14TMA	− 70.1 ± 1.6	1.097	1.14	1.097	3.899	0.04
18TMA	− 81.4 ± 1.7	1.007	1.034	0.996	2.689	1.107
TM322	− 51.3 ± 1.5	1.330	1.374	1.323	3.324	0.552

combined with adaptable calibrations can enhance the accuracy of values reported and minimize systematic effects induced by static calibration protocols [25].

Acknowledgements

References

1. Revercomb, H.E., Mason, E.A.: Theory of plasma chromatography/ gaseous electrophoresis- a review. Anal. Chem. **47**, 970–983 (1975)
2. Spangler, G.E., Collins, C.I.: Peak shape analysis and plate theory for plasma chromatography. Anal. Chem. **47**, 403–407 (1975)
3. Tabrizchi, M.: Temperature corrections for ion mobility spectrometry. Appl. Spectrosc. **55**, 1653–1659 (2001)
4. Kim, S.H., Betty, K.R., Karasek, F.W.: Mobility behavior and composition of hydrated positive reactant ions in plasma chromatography with nitrogen carrier gas. Anal. Chem. **50**, 2006–2012 (1978)
5. Eiceman, G.A., Nazarov, E.G., Stone, J.A.: Chemical standards in ion mobility spectrometry. Anal. Chim. Acta. **493**, 185–194 (2003)
6. Eiceman, G.A., Karpas, Z., Hill, H.H.J.: Ion Mobility Spectrometry. Taylor & Francis Group, Boca Raton, FL (2014)
7. McKnight, L.G., McAfee, K.B., Sipler, D.P.: Low-field drift velocities and reactions of nitrogen ions in nitrogen. Phys. Rev. **164**, 62–70 (1967)
8. Caygill, J.S., Davis, F., Higson, S.P.J.: Current trends in explosive detection techniques. Talanta. **88**, 14–29 (2012)
9. Ewing, R.G., Atkinson, D.A., Eiceman, G.A., Ewing, G.J.: A critical review of ion mobility spectrometry for the detection of explosives and explosive related compounds. Talanta. **54**, 515–529 (2001)
10. Uetrecht, C., Rose, R.J., van Duijn, E., Lorenzen, K., Heck, A.J.R.: Ion mobility mass spectrometry of proteins and protein assemblies. Chem. Soc. Rev. **39**, 1633–1655 (2010)
11. McLean, J.A., Ruotolo, B.T., Gillig, K.J., Russell, D.H.: Ion mobility-mass spectrometry: a new paradigm for proteomics. Int. J. Mass Spectrom. **240**, 301–315 (2005)
12. Fernandez-Lima, F., Kaplan, D.A., Suetering, J., Park, M.A.: Gas-phase separation using a trapped ion mobility spectrometer. Int. J. Ion Mobil. Spectrom. **14**, 93–98 (2011)
13. Fernandez-Lima, F.A., Kaplan, D.A., Park, M.A.: Note: integration of trapped ion mobility spectrometry with mass spectrometry. Rev. Sci. Instrum. **82**, (2011). https://doi.org/10.1063/1.3665933
14. Hernandez, D.R., DeBord, J.D., Ridgeway, M.E., Kaplan, D.A., Park, M.A., Fernandez-Lima, F.: Ion dynamics in a trapped ion mobility spectrometer. Analyst. **139**, 1913–1921 (2014)
15. Silveira, J.A., Ridgeway, M.E., Park, M.A.: High resolution trapped ion mobility spectrometery of peptides. Anal. Chem. **86**, 5624–5627 (2014)
16. Michelmann, K., Silveira, J.A., Ridgeway, M.E., Park, M.A.: Fundamentals of trapped ion mobility spectrometry. J. Am. Soc. Mass Spectrom. **26**, 14–24 (2014)
17. Silveira, J.A., Michelmann, K., Ridgeway, M.E., Park, M.A.: Fundamentals of trapped ion mobility spectrometry part II: fluid dynamics. J. Am. Soc. Mass Spectrom. **27**, 585–595 (2016)
18. Ridgeway, M.E., Lubeck, M., Jordens, J., Mann, M., Park, M.A.: Trapped ion mobility spectrometry: a short review. Int. J. Mass Spectrom. **425**, 22–35 (2018)
19. Silveira, J.A., Ridgeway, M.E., Laukien, F.H., Mann, M., Park, M.A.: Parallel accumulation for 100% duty cycle trapped ion mobility-mass spectrometry. Int. J. Mass Spectrom. **413**, 168–175 (2017)
20. Meier, F., Beck, S., Grassl, N., Lubeck, M., Park, M.A., Raether, O., Mann, M.: Parallel accumulation-serial fragmentation (PASEF): multiplying sequencing speed and sensitivity by synchronized scans in a trapped ion mobility device. J. Proteome Res. **14**, 5378–5387 (2015)
21. McKenzie-Coe, A., DeBord, J.D., Ridgeway, M., Park, M., Eiceman, G., Fernandez-Lima, F.: Lifetimes and stabilities of familiar explosive molecular adduct complexes during ion mobility measurements. Analyst. **140**, 5692–5699 (2015)
22. Benigni, P., Bravo, C., Quirke, M.J.E., DeBord, J.D., Mebel, A.M., Fernandez-Lima, F.: Analysis of geologically relevant metal porphyrins using trapped ion mobility spectrometry−mass spectrometry and theoretical calculations. Energy and Fuels. **30**, 10341–10347 (2016)
23. Jeanne Dit Fouque, K., Garabedian, A., Porter, J., Baird, M., Pang, X., Williams, T.D., Li, L., Shvartsburg, A., Fernandez-Lima, F.: Fast and effective ion mobility - mass spectrometry separation of D-amino acid containing peptides. Anal. Chem. acs.analchem.7b03401 (2017)
24. Liu, F.C., Kirk, S.R., Bleiholder, C.: On the structural denaturation of biological analytes in trapped ion mobility spectrometry – mass spectrometry. Analyst. **141**, 3722–3730 (2016)
25. Chai, M., Young, M.N., Liu, F.C., Bleiholder, C.: A transferable, sample-independent calibration procedure for trapped ion mobility spectrometry (TIMS). Anal. Chem. (2018). https://doi.org/10.1021/acs.analchem.8b01326
26. Stow, S.M., Causon, T.J., Zheng, X., Kurulugama, R.T., Mairinger, T., May, J.C., Rennie, E.E., Baker, E.S., Smith, R.D., McLean, J.A., Hann, S., Fjeldsted, J.C.: An interlaboratory evaluation of drift tube ion mobility-mass spectrometry collision cross section measurements. Anal. Chem. **89**, 9048–9055 (2017)
27. Ewing, R.G., Eiceman, G.A., Harden, C.S., Stone, J.A.: The kinetics of the decompositions of the proton bound dimers of 1,4-dimethylpyridine and dimethyl methylphosphonate from atmospheric pressure ion mobility spectra. Int. J. Mass Spectrom. **255-256**, 76–85 (2006)
28. Karpas, Z., Berant, Z., Shahal, O.: Effect of temperature on the mobility of ions. J. Am. Chem. Soc. **111**, 6015–6018 (1989)
29. Abedi, A., Sattar, L., Gharibi, M., Viehland, L.A.: Investigation of temperature, electric field and drift-gas composition effects on the mobility of $NH4+$ions in He, Ar, N2, and CO2. Int. J. Mass Spectrom. **370**, 101–106 (2014)
30. Demoranville, L.T., Houssiau, L., Gillen, G.: Behavior and evaluation of tetraalkylammonium bromides as instrument test materials in thermal desorption ion mobility spectrometers. Anal. Chem. **85**, 2652–2658 (2013)
31. Ude, S., De La Mora, J.F.: Molecular monodisperse mobility and mass standards from electrosprays of tetra-alkyl ammonium halides. J. Aerosol Sci. **36**, 1224–1237 (2005)
32. Viidanoja, J., Sysoev, A., Adamov, A., Kotiaho, T.: Tetraalkylammonium halides as chemical standards for positive electrospray ionization with ion mobility spectrometry/mass spectrometry. Rapid Commun. Mass Spectrom. **19**, 3051–3055 (2005)
33. May, J.C., Goodwin, C.R., Lareau, N.M., Leaptrot, K.L., Morris, C.B., Kurulugama, R.T., Mordehai, A., Klein, C., Barry, W., Darland, E., Overney, G., Imatani, K., Stafford, G.C., Fjeldsted, J.C., McLean, J.A.: Conformational ordering of biomolecules in the gas phase: nitrogen collision cross sections measured on a prototype high resolution drift tube ion mobility-mass spectrometer. Anal. Chem. **86**, 2107–2116 (2014)
34. Haler, J.R.N., Kune, C., Massonnet, P., Comby-Zerbino, C., Jordens, J., Honing, M., Mengerink, Y., Far, J., De Pauw, E.: Comprehensive ion mobility calibration: poly(ethylene oxide) polymer calibrants and general strategies. Anal. Chem. **89**, 12076–12086 (2017)
35. Gidden, J., Wyttenbach, T., Jackson, A.T., Scrivens, J.H., Bowers, M.T.: Gas-phase conformations of synthetic polymers: poly(ethylene glycol), poly(propylene glycol), and poly(tetramethylene glycol). J. Am. Chem. Soc. **122**, 4692–4699 (2000)
36. Wyttenbach, T., Pierson, N.A., Clemmer, D.E., Bowers, M.T.: Ion mobility analysis of molecular dynamics. Annu. Rev. Phys. Chem. **65**, 175–196 (2014)
37. Shumate, C., St.Louis, R.H., Hill, H.H., Jr.: Table of reduced mobility ion mobility spectrometry values from ambient. J. Chromatogr. A. 373, 141–173 (1986)
38. May, J.C., Morris, C.B., McLean, J.A.: Ion mobility collision cross section compendium. Anal. Chem. **89**, 1032–1044 (2017)
39. Li, H., Bendiak, B., Siems, W.F., Gang, D.R., Hill Jr., H.H.: Carbohydrate structure characterization by tandem ion mobility mass spectrometry (IMMS)2. Anal. Chem. **85**, 2760–2769 (2013)
40. Reinecke, T., Clowers, B.H.: Implementation of a flexible, open-source platform for ion mobility spectrometry. HardwareX. 4, (2018). doi:https://doi.org/10.1016/j.ohx.2018.e00030

41. Langejuergen, J., Allers, M., Oermann, J., Kirk, A., Zimmermann, S.: High kinetic energy ion mobility spectrometer: quantitative analysis of gas mixtures with ion mobility spectrometry. Anal. Chem. **86**, 7023–7032 (2014)

42. Reinecke, T., Kirk, A.T., Ahrens, A., Raddatz, C.R., Thoben, C., Zimmermann, S.: A compact high resolution electrospray ionization ion mobility spectrometer. Talanta. **150**, 1–6 (2016)

43. Garcia, L., Saba, C., Manocchio, G., Anderson, G.A., Davis, E., Clowers, B.H.: An open source ion gate pulser for ion mobility spectrometry. Int. J. Ion Mobil. Spectrom. **20**, 87–93 (2017)

44. Hauck, B.C., Siems, W.F., Harden, C.S., McHugh, V.M., Hill, H.H.: Determination of E/N influence on K_0 values within the low field region of ion mobility spectrometry. J. Phys. Chem. A. 1, acs.jpca.6b12331 (2017)

45. Reinecke, T.: MP 397 Development of a High Performance, Modular Ion Mobility Spectrometer using Printed Circuit Boards. 66th ASMS Conference on Mass Spectrometry and Allied Topics. , San Diego Convention Center, San Diego, CA, USA (2018)

46. Clowers, B.H., Hill, H.H.: Mass analysis of mobility-selected ion populations using dual gate, ion mobility, quadrupole ion trap mass spectrometry. Anal. Chem. **77**, 5877–5885 (2005)

47. Morrison, K.A., Siems, W.F., Clowers, B.H.: Augmenting ion trap mass spectrometers using a frequency modulated drift tube ion mobility spectrometer. Anal. Chem. **88**, 3121–3129 (2016)

48. Hauck, B.C., Siems, W.F., Harden, C.S., McHugh, V.M., Hill, H.H.: E/N effects on K0 values revealed by high precision measurements under low field conditions. Rev. Sci. Instrum. **87**, 075104 (2016)

49. Hauck, B.C., Siems, W.F., Harden, C.S., McHugh, V.M., Hill, H.H.: High accuracy ion mobility spectrometry for instrument calibration. Anal. Chem. **90**, 4578–4584 (2018)

50. Baker, E.S., Clowers, B.H., Li, F., Tang, K., Tolmachev, A.V., Prior, D.C., Belov, M.E., Smith, R.D.: Ion mobility spectrometry-mass spectrometry performance using electrodynamic ion funnels and elevated drift gas pressures. J. Am. Soc. Mass Spectrom. **18**, 1176–1187 (2007)

51. Davis, A.L., Liu, W., Siems, W.F., Clowers, B.H.: Correlation ion mobility spectrometry. Analyst. **142**, 292–301 (2017)

52. Davis, A.L.: Multiplexing techniques applied to ion mobility measurements. Ph.D. Dissertation, Washington State University (2018)

53. Reinecke, T., Davis, A.L., Clowers, B.H.: Determination of gas-phase ion mobility coefficients using voltage sweep multiplexing. J. Am. Soc. Mass Spectrom. 30, 977–986 (2019)